Journal of Non-Newtonian Fluid Mechanics 327 (2024) 105220

Contents lists available at ScienceDirect

Journal of Non-Newtonian Fluid Mechanics

journal homepage: www.elsevier.com/locate/jnnfm

Full Length Article

Modeling Elongational Rheology of Model Poly((±)-lactide) Graft Copolymer Bottlebrushes☆

Manfred H. Wagner [a,*], Aristotelis Zografos [b], Valerian Hirschberg [c,d]

[a] Polymer Engineering/Polymer Physics, Berlin Institute of Technology (TU Berlin), Ernst-Reuter-Platz 1, 10587, Berlin, Germany
[b] Department of Chemical Engineering and Materials Science, University of Minnesota, Minneapolis, MN, 55455-0132, United States
[c] Institute of Chemical Technology and Polymer Chemistry (ITCP), Karlsruhe Institute of Technology (KIT), Engesserstraße 18, 76131, Karlsruhe, Germany
[d] Institute for Technical Chemistry, Technical University Clausthal, Arnold-Sommerfeld-Str. 4, 38678, Clausthal-Zellerfeld, Germany

ARTICLE INFO

Keywords:
Bottlebrush polymers
Comb polymers
Branching
Elongational viscosity
Strain hardening
Dynamic dilution
HMMSF model
Hyperstretching

ABSTRACT

The shear and elongational rheology of graft polymers with poly(norbornene) backbone and one poly((±)-lactide) side chain of length $N_{sc} = 72$ per two backbone repeat units (grafting density $z = 0.5$) was investigated recently by Zografos et al. [Macromolecules 56, 2406–2417 (2023)]. Above the star-to-bottlebrush transition at backbone degrees of polymerization of $N_{bb}>70$, increasing strain hardening was observed with increasing N_{bb}, which was attributed to side-chain interdigitation resulting in enhanced friction in bottlebrush polymers. Here we show that the elongational rheology of the copolymers with entangled side chains and an unentangled backbone can be explained by the Hierarchical Multi-mode Molecular Stress Function (HMMSF) model, which takes into account hierarchical relaxation and dynamic dilution of the backbone by the side chains, leading to constrained Rouse relaxation. In nonlinear viscoelastic flows with larger Weissenberg numbers, the effect of dynamic dilution is increasingly reduced leading to stretch of the backbone chain caused by side chain constraints and resulting in strain hardening. If the backbone is sufficiently long, hyperstretching is observed at larger strain rates, i.e. the stress growth is greater than expected from affine stretch.

1. Introduction

Bottlebrush polymers are comb polymers with a high graft density along their backbone. Comb and bottlebrush polymers show strong strain hardening in elongational flow, which depends on the backbone and side chain lengths as well as the number of branches per molecule or the grafting density [1]. Strain hardening as, e.g., defined and discussed in detail by Dealy and Larson [2], is of special interest to industrial applications like film blowing, fiber spinning and foaming; and transient strain hardening refers to the upward deviation of the elongational stress growth coefficient from the linear-viscoelastic (LVE) envelop. McLeish and Larson [3] showed that at least two long-chain branches (LCB) per molecule are needed to induce strain hardening. Abbasi and coworkers [4] investigated the impact of the number of LCB branches from loosely grafted combs to bottlebrushes and showed that the strain hardening factor (SHF) increases significantly with increasing number of branches. López-Barrón and coworkers [5,6] observed substantial transient strain hardening of the elongational stress growth coefficient of poly(α-olefin) bottlebrushes, and attributed this to an increase in side-chain interdigitation as soon as the polymers align in the flow direction. The shear and elongational rheology of graft polymers with poly(norbornene) backbone and poly((±)-lactide) side chains was investigated recently by Zografos et al. [7]. Above the star-to-bottlebrush transition, increasing strain hardening was observed with increasing backbone degree of polymerization, which was ascribed again to side-chain interdigitation resulting in enhanced chain friction and strain hardening.

In a recent analysis, Wagner and Hirschberg [8] have shown that the elongational rheology of the poly(α-olefin) bottlebrushes investigated by López-Barrón and coworkers [5,6] with entangled backbone and unentangled side chains can be explained by self-dilution of the backbone by the alkane side chains. The rheology of poly(α-olefins) is similar to the rheology of high molecular weight linear polymers diluted in oligomers of the same chemistry as described by the Enhanced Relaxation of Stress (ERS) model [9]. In contrast to the poly(α-olefin) bottlebrushes, the polylactide (PLA) copolymers synthesized by Zografos et al. [7] have entangled poly((±)-lactide) side chains and an unentangled

☆ Dedicated to the memory of Prof. John M. Dealy (1937–2024)

* Corresponding author.
E-mail address: manfred.wagner@tu-berlin.de (M.H. Wagner).

https://doi.org/10.1016/j.jnnfm.2024.105220
Received 21 February 2024; Received in revised form 16 March 2024; Accepted 19 March 2024
Available online 20 March 2024

Table I
Molecular characterization of model poly((±)-lactide) graft copolymers: Number N_{bb} of backbone repeat units, weight average molecular weight M_w, polydispersity M_w/M_n, plateau modulus G_N^0, zero-shear viscosity η_0 and disengagement time τ_d at T_{ref} =86 °C. All graft copolymers have graft density z = 0.5 and the same number N_{sc}=72 of side-chain (±)-lactide repeat units.

Copolymer N_{bb}	M_w [kg/mol]	M_w/M_n [-]	G_N^0 [kPa]	η_0 [kPas]	τ_d [s]
Macromonomer (N_{sc}=72)	10.5	–	700	5.42	0.0097
50	266	1.01	700	82.5	0.68
110	562	1.03	700	126	4.15
160	828	1.04	n.d.	200	11.8
200	1080	1.04	600	230	17.6
320	1740	1.04	610	417	74.4
420	2240	1.18	560	577	207

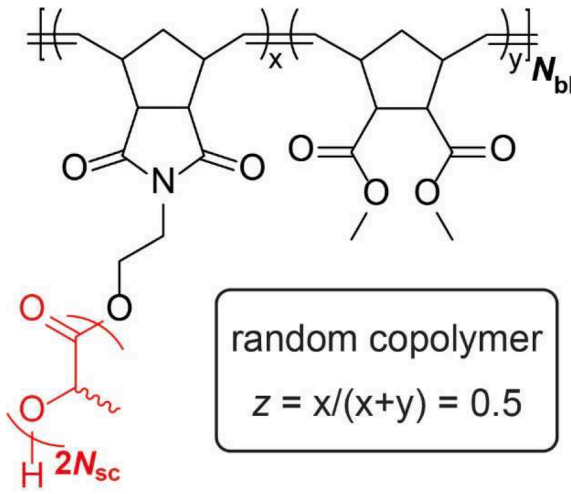

Fig. 1. Model poly(norbornene/lactide) copolymers [7].

poly(norbornene) backbone. In this contribution we show that the elongational rheology of the PLA copolymers can be described by the Hierarchical Multi-mode Molecular Stress Function (HMMSF) model [10–15], which considers hierarchical relaxation and dynamic dilution of the backbone by the side chains. We first summarize the molecular and linear-viscoelastic characterization of the poly(norbornene/lactide) copolymers. We then give a short summary of the HMMSF model with hyperstretching, which has recently been introduced to model the elongational rheology of a series of comb to bottlebrush polystyrene (PS) model polymers [15], followed by a comparison of experimental data and model predictions.

2. Molecular and linear-viscoelastic characterization of model poly((±)-lactide) graft copolymers

The molecular properties of the poly(norbornene/lactide) copolymers are taken from Zografos et al. [7] and are summarized in Table I. Poly((±)-lactide) ω-norbornenyl macromonomer (MM) was copolymerized with a dimethyl-ester norbornene (DME) comonomer, yielding graft polymers with a poly(norbornene) backbone and poly((±)-lactide) side chains (Fig.1), and one graft for every two backbone repeat units ($z = 0.5$). The number of (±)-lactide repeat units was held constant at N_{sc}=72, the number of backbone repeat units was varied between N_{bb}= 11 and 420. The star-like to bottlebrush transition was identified at N_{bb}=50 to 70 using small amplitude oscillatory shear (SAOS) rheometry. We restrict attention here to the macromonomer sample (MM) and the copolymers tested by Zografos and coworkers in elongational rheometry, namely the star-like copolymer with N_{bb}=50 and the bottlebrush copolymers with N_{bb}=110, 160, 220, 320, and 420.

For characterization of the linear viscoelasticity (LVE) of all copolymers considered here, we obtained discrete relaxation time spectra for the relaxation modulus

$$G(t) = \sum_i G_i(t) = \sum_i g_i \exp(t/\tau_i) \quad (1)$$

from the mastercurves of storage modulus (G') and loss modulus (G'') as reported by Zografos et al. [7] at the reference temperature T_{ref}=86 °C. The partial moduli g_i and relaxation times τ_i as determined by the IRIS software [16,17] resulted in excellent agreement with the linear-viscoelastic data of G' and G'' and are reported in the supplementary material (SM). We take the plateau modulus G_N^0 as the value of the storage modulus G' at the high frequency G' minimum of the loss tangent δ (Fig.2a). We calculated the zero-shear viscosity η_0 and the mean quadratic average of the relaxation time, which we take as "disengagement" time τ_d[2] and as reference time scale of the LVE relaxation process, by

$$\eta_0 = \sum_i g_i \tau_i \quad (2)$$

and

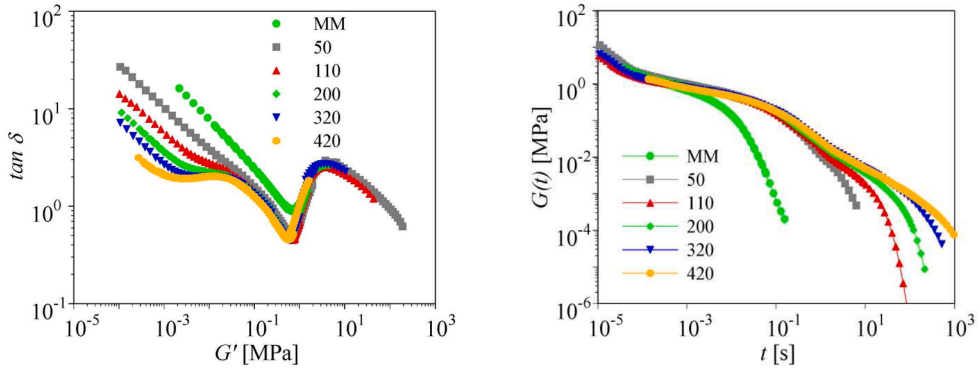

Fig. 2. (a) Loss tangent δas a function of storage modulus G'. (b) Relaxation modulus $G(t)$ at the reference temperature T_{ref}=86 °C. From top to bottom: MM, copolymers with N_{bb}=50, 110, 200, 320, and 420.

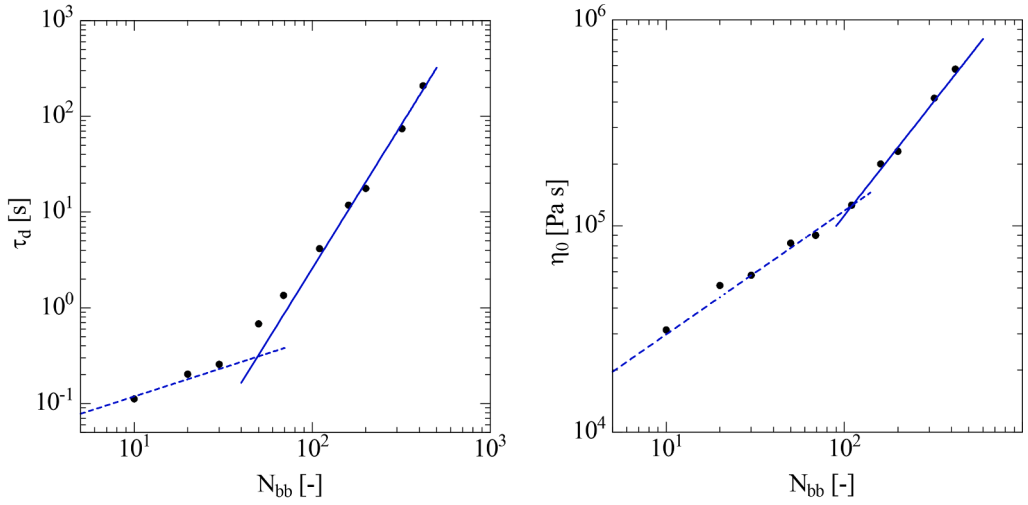

Fig. 3. Disengagement time τ_d(a) and zero-shear viscosity η_0 (b) as a function of backbone repeat units N_{bb} at $T = 86$ °C. Broken line indicates power-law with exponent of $a = 0.6$, continuous line power-law with exponent of $a = 3$ (a) and $a = 1.1$ (b), respectively.

$$\tau_d = \frac{\sum_i g_i \tau_i^2}{\sum_i g_i \tau_i} \tag{3}$$

For the poly((±)-lactide) ω-norbornenyl macromonomer (MM) we calculated the entanglement molecular weight M_e at T_{ref} by

$$M_e = \frac{\rho RT}{G_N^0} \tag{4}$$

ρ is the density, R the gas constant, and $T = 273K + T_{ref}$ the absolut temperture. According to Witzke [18], the liquid or melt density of L-, *meso* LA-, and amorphous LA-lactide can be expressed by $\rho = 1.2836\exp(-7.7{\cdot}10^{-4}T_{ref}) = 1.201 g/cm^3$ (with T_{ref} in °C). Assuming that the density of the MM is the same as the density of lactide, a value of M_e=5.1 *kg/mol* is obtained from Eq. (4). With M_w=10.5 *kg/mol*, the MM can be considered as marginally entangled, which corresponds to the minimum value of the loss tangent $\delta = 0.88$. However, as seen from Fig. 2a, the poly((±)-lactide) graft copolymers appear well entangled with the minimum of the loss tangent δ being significantly below a value of *1* (Fig.2a), i.e. the graft copolymers have a well-defined rubber-like plateau, as also seen in the relaxation modulus *G(t)* (Fig.2b). In the graft copolymers, the poly((±)-lactide) side chains are tethered to the backbone and cannot relax by reptation, but relax by arm retraction and by constraint release. Arm retraction scales exponentially with molecular weight, making the relaxation process much slower than reptation. This is why the well-defined plateau-like region is seen for the graft copolymers in Fig.2 and not for the macromonomer. The breadth of the plateau does not change as the number of backbone repeat units and therefore the number of side-chains increases, because the arm relaxation time does not depend on the number of arms present. At values of N_{bb} of 110 or larger, a distinct kink in the tanδ curve is observed at lower values of *G'*, which progresses to a shallow minimum of the loss tangent δ with a value 1.9 at $G' \cong 3$ *kPa* for N_{bb}=420 (Fig.2a). This kink is also seen in the relaxation modulus *G(t)* (Fig.2b). There is no self-entanglement of the poly(norbornene) backbones with $N_{bb} \leq 420$, i.e. there are no direct backbone-backbone entanglements due to dilution by the side chains to a backbone weight fraction of $\phi_{bb} = 0.04$. Instead, the relaxation of the backbones is constrained by the entangled poly((±)-lactide) side chains. The backbone chains relax by constraint release of the side chains, and on longer time scales corresponding to lower frequencies in small amplitude oscillatory shear (SAOS), there are fewer and fewer constraints remaining until eventually the poly(norbornene) backbone chains reach the terminal relaxation regime on the time scale of the longest relaxation time. The relaxation process is facilitated by dynamic dilution, i.e. the already relaxed poly((±)-lactide) side chains act as diluent for the chains not yet relaxed [2]. As shown in Fig.3, the disengagement time τ_d increases with increasing number N_{bb} of backbone repeat units and therefore the length of the backbone. For $N_{bb}<50$, τ_d increases by a power-law with $\tau_d \propto N_{bb}^a$ and exponent of $a = 0.6$, while after the star to bottlebrush transition and for $N_{bb} \geq 100$, the exponent is $a = 3$. For melts of unentangled polymer chains, Rouse scaling with an exponent of $a = 2$ would be expected. The exponent of $a = 3$ is a signature of the additional effect of the entangled side chains. The zero-shear viscosity inceases initially also by a power-law with $\eta_0 \propto N_{bb}^a$ and exponent of $a = 0.6$, but for $N_{bb} \geq 100$, the exponent is found to be approximately equal to $a = 1.1$ [7]. For unentangled Rouse melts, a linear relation between viscosity and N_{bb} (or molecular weight) is expected, and thus, the terminal relaxation of the bottlebrush copolymers is dominated by constrained Rouse relaxation. This is shown in Fig. 4 for the copolymer with N_{bb}=320: The terminal relaxation of *G'* follows Rouse scaling with Rouse time τ_R=104 s for about 3 decades in

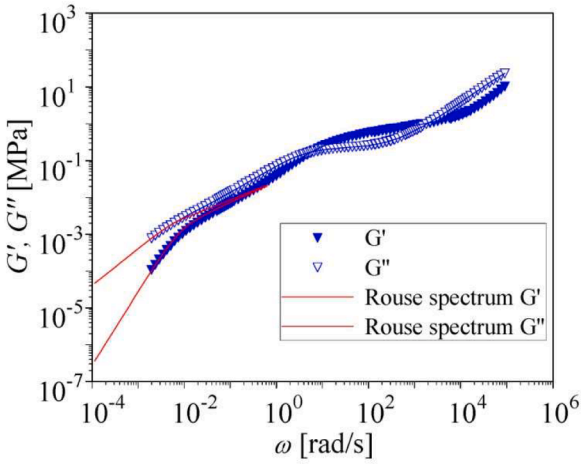

Fig. 4. Storage (G') and loss modulus (G'') of copolymer with N_{bb}=320 (symbols). Lines represent G' and G'' of Rouse relaxation time spectrum with Rouse relaxation time τ_R=104 s and modulus G_R=2.4 kPa.

frequency, from $\omega = 1$ down to the lowest frequency measured at $\omega = 10^{-3}\ s^{-1}$.

3. Hierarchical Multi-mode Molecular Stress Function (HMMSF) model with hyperstretching

The HMMSF model takes hierarchical relaxation and dynamic dilution of temporary network strands into account as shortly summarized here. The extra stress tensor of the HMMSF model is given by [10–12],

$$\sigma(t) = \sum_i \int_{-\infty}^{t} \frac{\partial G_i(t-t')}{\partial t'} f_i^2(t,t') \mathbf{S}_{DE}^{IA}(t,t') dt' \tag{5}$$

The network strands are characterized by their partial relaxation moduli $G_i(t)$ according to Eq. (1), and by the molecular stress functions f_i. In this way, the effect of relaxation and stretch of side arms and of backbone chains and their complex topological interaction is mapped onto virtual temporary network strands. The strain measure $\mathbf{S}_{DE}^{IA}$ represents the contribution to the extra stress tensor originating from the affine rotation of network strands according to the "Independent Alignment (IA)" assumption of Doi and Edwards [19,20], and is given by

$$\mathbf{S}_{DE}^{IA}(t,t') \equiv 5\left\langle \frac{\mathbf{u}'\mathbf{u}'}{u'^2} \right\rangle_o = 5\mathbf{S}(t,t') \tag{6}$$

with $\mathbf{S}(t,t')$ being the relative second order orientation tensor. $\mathbf{u}'\mathbf{u}'$ is the dyad of a deformed unit vector $\mathbf{u}' = \mathbf{u}'(t,t')$,

$$\mathbf{u}' = \mathbf{F}_t^{-1} \cdot \mathbf{u} \tag{7}$$

$\mathbf{F}_t^{-1} = \mathbf{F}_t^{-1}(t,t')$ is the relative deformation gradient tensor, and u' is the length of $\mathbf{u}'$. The orientation average is indicated by $<\ldots>_0$,

$$\langle \ldots \rangle_o \equiv \frac{1}{4\pi} \int\int [\ldots] \sin\theta_o d\theta_o d\phi_o \tag{8}$$

i.e. an average over an isotropic distribution of unit vectors $\mathbf{u}$.

The molecular stress functions $f_i = f_i(t,t')$ in Eq.(5) are given by,

$$f_i(t,t') = \frac{l_i(t,t')}{l_{i0}} \tag{9}$$

with l_{i0} being the equilibrium length of the network strands of mode i. The molecular stress functions $f_i = f_i(t,t')$ are functions of both the observation time t and the time t' of creation of strands by diffusion. We note for later use that for $f_i \equiv 1$, Eq. (5) reduces to the Doi-Edwards IA equation [19,20].

Restricting attention to comb and bottlebrush polymers in extensional flows and accounting for the effects of stretch relaxation [12,15], which in the case of LCB polymers depends on the relaxation times τ_i and not the Rouse time of the chain, the evolution equation for the molecular stress function f_i of each mode i can be expressed as,

$$\frac{\partial f_i}{\partial t} = (1+k) f_i (\mathbf{K} : \mathbf{S}) - \frac{f_i - 1}{\tau_i}\left(1 - w_i^2\right) - \frac{\left(f_i^5 - 1\right)}{5\tau_i} w_i^2 \tag{10}$$

with the initial conditions $f_i(t = t', t') = 1$. The first term on the right-hand side represents the hyperstretching rate with $\mathbf{K}$ being the velocity gradient. k is the hyperstretch factor with $0 \le k \le 1$, which considers that in the case of densely grafted polymer combs, there are several branch points per entanglement length of the backbone, causing additional topological constraints on length scales smaller than the entanglement length and, therefore, creating extra tension as explained by Hirschberg et al. [15]. The second term takes into account stretch relaxation, and the third term limits stretch due to enhanced relaxation of stretch on smaller length scales as shown in [9], leading to a stretch relaxation term which is proportional to the 5th power of the stretch f_i.

The stretch relaxation terms of Eq. (10) depend on the weight fractions w_i of the relaxation modes, and account for hierarchical relaxation and dynamic dilution, because relaxation modes with shorter relaxation times dilute those with longer relaxation times as, e.g., explained by Dealy and Larson [2]. The weight fractions w_i can be derived from the linear-viscoelastic relaxation time spectrum in the following way [10,11]: We distinguish between two dilution regimes during the relaxation process, the regime of permanent dilution, and the regime of dynamic dilution. Permanent dilution occurs due to the presence of oligomeric chains and unentangled (fluctuating) chain ends. We assume that the onset of dynamic dilution starts as soon as the relaxation process has reached a specific relaxation modulus, the so-called dilution modulus $G_D \le G_N^0$. The dilution modulus G_D is a free parameter of the model,

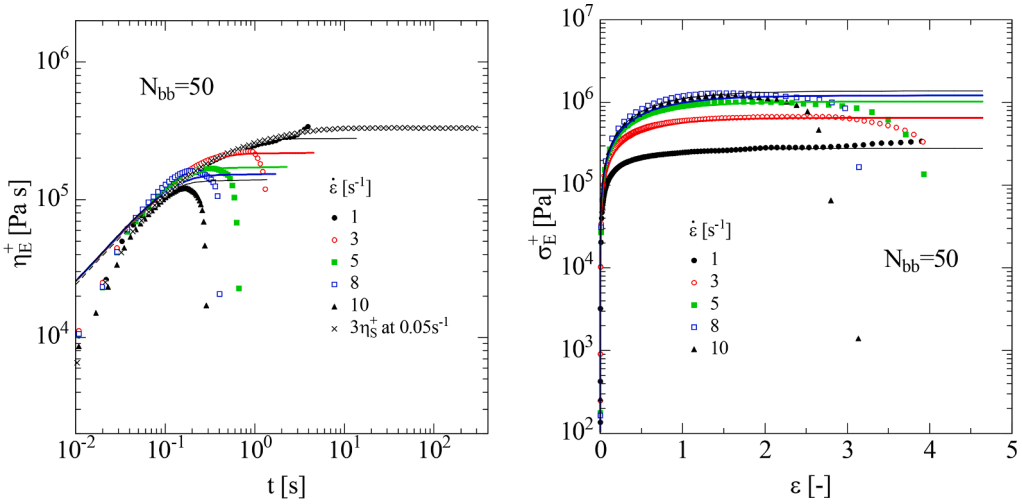

(a) (b)

Fig. 5. Comparison of (a) the elongational stress growth coefficient $\eta_E^+(t)$ and (b) the elongational stress growth $\sigma_E^+(\varepsilon)$ data (symbols) at T_e=85 °C to calculated results of the Doi-Edwards IA model (lines) for copolymer with N_{bb}=50.

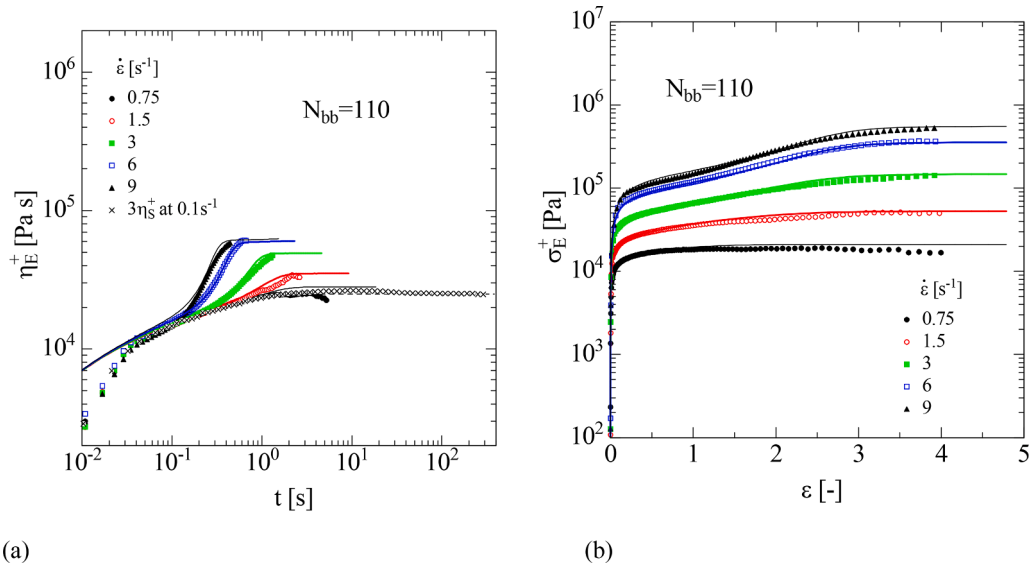

(a) (b)

Fig. 6. Comparison of (a) the elongational stress growth coefficient $\eta_E^+(t)$ and (b) the elongational stress growth $\sigma_E^+(\varepsilon)$ data (symbols) at T_e=100 °C to calculated results of the HMMSF model (lines) with dilution modulus G_D=40 kPa and without hyperstretching ($k = 0$) for copolymer with N_{bb}=110.

which needs to be fitted to non-linear viscoelastic experimental evidence, since the mass fraction of oligomeric chains and the effect of unentangled and/or fluctuating chain ends is in general not known a-priori. At time $t = \tau_D$ the relaxation modulus $G(t)$ has relaxed to the value of G_D and dynamic dilution starts, while at relaxation times $t \leq \tau_D$, the chain segments are assumed to be permanently diluted. Hence, the dilution modulus G_D separates the zone of permanent dilution from the zone of dynamic dilution. The weight fraction w_i of dynamically diluted network strands with relaxation time $\tau_i > \tau_D$ is determined by considering the ratio of the relaxation modulus at time $t = \tau_i$ to the dilution modulus G_D,

$$w_i^2 = \frac{G(t=\tau_i)}{G_D} = \frac{1}{G_D}\sum_{j=1}^{n} g_j \exp(-\tau_i/\tau_j) \quad \text{for } \tau_i > \tau_D$$
$$w_i^2 = 1 \quad \text{for } \tau_i \leq \tau_D \tag{11}$$

The value of w_i obtained at $t = \tau_i$ is attributed to the relaxation mode with relaxation time τ_i. Relaxation modes with $\tau_i < \tau_D$ are considered to be permanently diluted, i.e. their weight fractions are fixed at $w_i = 1$. As shown by Narimissa et al. [21], these assumptions allow modeling the rheology of broadly distributed polymers, largely independent of the number of discrete Maxwell modes used to represent the relaxation modulus $G(t)$. We note that the values of the weight fractions w_i do not influence the onset of stretching, which can be seen by considering the limit of Eq.(10) for $f_i \to 1$, which is $\frac{\partial f_i}{\partial t} = (1+k) f_i(\mathbf{K}:\mathbf{S}) - \frac{f_i - 1}{\tau_i}$ [9]. However, the magnitude of strain hardening depends on the values of w_i and therefore G_D. Because $G(t)$ is a monotonously decreasing function of time t, the modes with the longest relaxation times τ_i experience the highest degree of dynamic dilution [21], which in nonlinear flow results in the highest molecular stress functions f_i according to Eq.(10).

4. Comparison of HMMSF model predictions and elongational viscosity data of poly((±)-lactide) graft copolymers

Zografos et al. [7] determined the elongational rheology of the copolymers with N_{bb}=50, 110, 160, 220, 320, and 420 at experiment

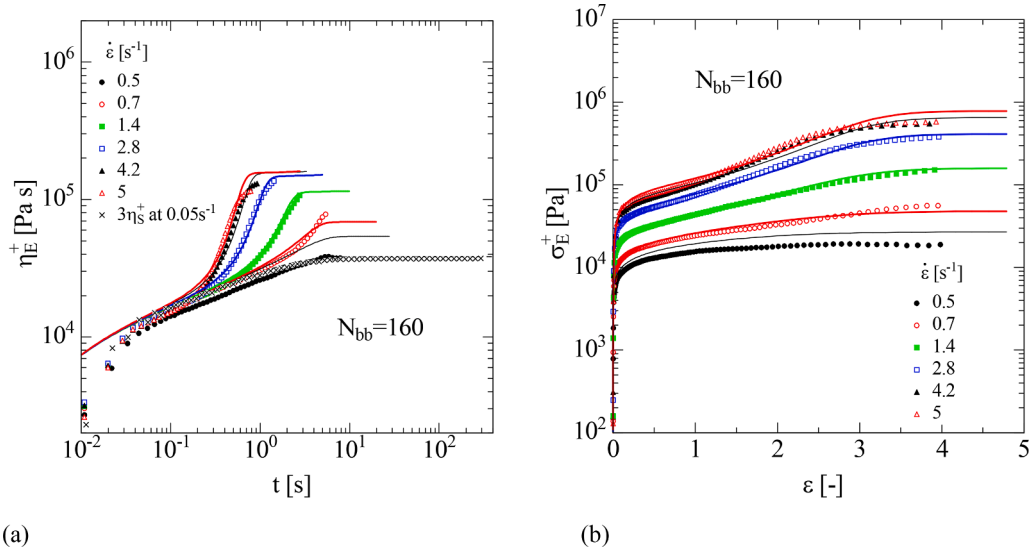

(a) (b)

Fig. 7. Comparison of (a) the elongational stress growth coefficient $\eta_E^+(t)$ and (b) the elongational stress growth $\sigma_E^+(\varepsilon)$ data (symbols) at T_e=100 °C to calculated results of the HMMSF model (lines) with dilution modulus G_D=90 kPa and without hyperstretching ($k = 0$) for copolymer with N_{bb}=160.

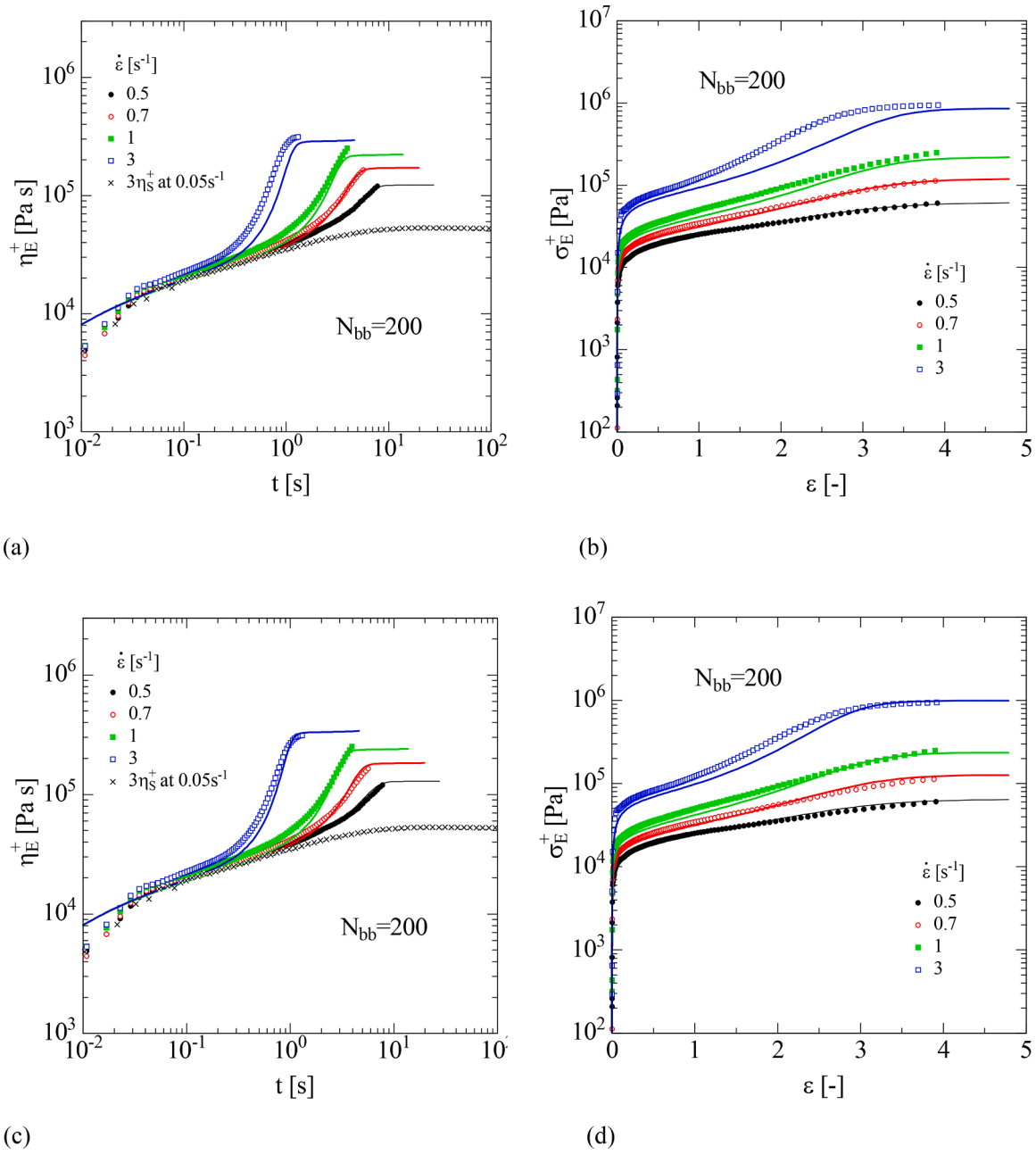

Fig. 8. Comparison of (a and c) the elongational stress growth coefficient $\eta_E^+(t)$ and (b und d) the elongational stress growth $\sigma_E^+(\varepsilon)$ data (symbols) at T_e=100 °C to calculated results of the HMMSF model (lines) with dilution modulus G_D=150 kPa, without hyperstretching ($k = 0$) (a and b) and with hyperstretching (c and d) acccording to Eq.(12) for copolymer with N_{bb}=200.

temperatures T_e ranging from 86 to 110 °C using an EVF rheometer. The measurements were performed at Hencky strain rates up to the maximal strain rate possible without sample fracture, or up to a maximum strain rate of $\dot{\varepsilon} = 10\ s^{-1}$, i.e., the maximum strain rate that can be applied. Samples were stretched up to a Hencky strain of $\varepsilon = 4$, which is the maximum strain possible without wrapping the sample back onto itself. The relaxation spectra were shifted to the experiment temperature T_e by use of the time-temperature shift (TTS) factors reported by Zografos et al. [7].

Predictions of the HMMSF model with stress tensor Eq. (5) and stretch evolution Eq. (10) are compared in Figs. 5 to 10 to the data (symbols) of the elongational stress growth coefficient $\eta_E^+(t)$ as a function of time t, and the elongational stress growth $\sigma_E^+(\varepsilon)$ as a function of Hencky strain ε as reported by Zografos et al. [7]. The data of 3 times the shear stress growth coefficient $\eta_s^+(t)$ are also shown, which were measured at shear rates suffienctly small to agree with the linear-viscoelastic start-up viscosity. The star-like copolymer with N_{bb}=50 shows a maximum in elongational stress at a Hencky strains of $\varepsilon \cong 1$, and does not show any significant strain hardening in the experimental window (Fig. 5). The decreasing viscosity and stress after the maximum are caused by inhomogeneous sample deformation. The elongational behavior of the copolymer with N_{bb}=50 up to the maximum of stress and viscosity is best described in the experimental window by the HMMSF model with $f_i \equiv 1$, i.e. the Doi-Edwards IA model [19,20], which takes only orientation into account.

In contrast to the star-like copolymer with N_{bb}=50, the bottlebrush copolymers with N_{bb}=110 (Fig.6) and N_{bb}=160 (Fig.7) show significant transient strain hardening, which can be described by the HMMSF model with a dilution modulus G_D of 40 kPa and 90 kPa, respectively. For these copolymer samples, there is no significant evidence of hyperstretching

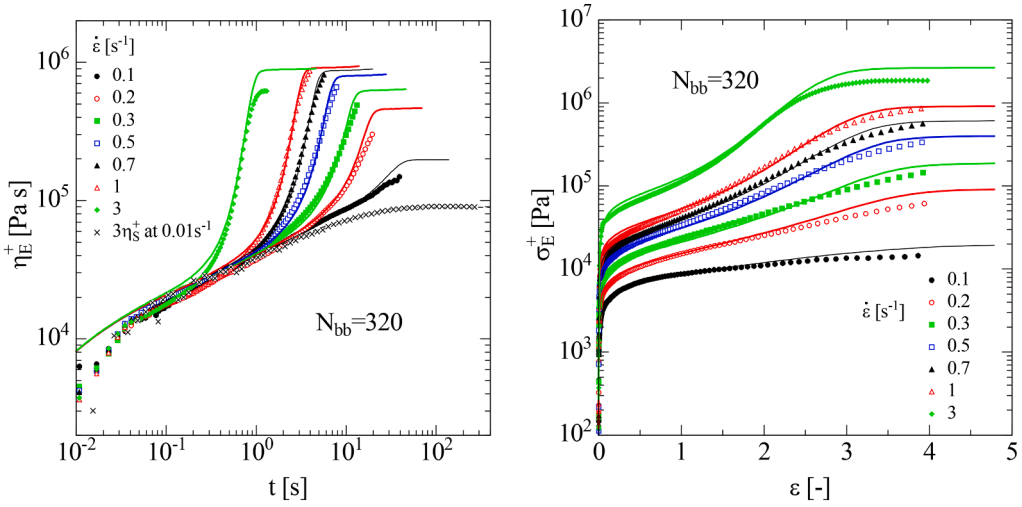

(a) (b)

Fig. 9. Comparison of (a) the elongational stress growth coefficient $\eta_E^+(t)$ and (b) the elongational stress growth $\sigma_E^+(\varepsilon)$ data (symbols) at T_e=100 °C to calculated results of the HMMSF model (lines) with dilution modulus G_D=180 kPa and with hyperstretching according to Eq.(12) for copolymer with N_{bb}=320.

in the experimental window of strain rates investigated, i.e. the experimental data are in agreement with $k = 0$ in the stretch evolution Eq. (10).

Enhanced transient strain hardening is observed for the copolymer with N_{bb}=200 (Fig. 8). While the HMMSF model with a dilution modulus G_D of 150 kPa and without hyperstretching ($k = 0$) results in description of the elongational data for the two low strain rates, deviation is seen at the two high strain rates investigated (Fig.8a,b). An improved modeling can be achieved by taking into account the effect of hyperstretching of the backbone at larger strain rates by assuming that the hyperstretch factor k changes with the Weissenberg number $Wi = \dot{\varepsilon}\tau_d$ according to

$$k = 1 - \exp(-0.06\, Wi_d) \tag{12}$$

This empirical relation guarantees that k approaches the maximal value of $k = 1$ for large Wi_d. A hyperstretch factor $k = 1$ was found to accurately describe the hyperstretching of polystyrene bottlebrush polymers in elongational flow [15]. However, in these investigations the limit of $Wi_d \to 0$ was not reached. In this limit, hyperstretching is expected to vanishing (i.e., $k = 0$) because at time scales larger than τ_d most of the side chains have relaxed and, therefore, do not contribute any more to this process. The relation (12) is in agreement with the elongational data of the copolymer with $N_{bb} = 200$ as shown in Figs. 8c, d, but also with those of the copolymers with $N_{bb} = 320$ and 420 as shown below.

For the copolymer sample with $N_{bb} = 320$ (Fig.9), the optimal value of the dilution modulus is G_D=180 kPa, while for the copolymer with N_{bb}=420 (Fig.10), it is G_D=250 kPa. We note that for PS homopolymer combs and bottlebrushes, the dilution modulus was found to be identical to the plateau modulus [13–15]. As we consider a copolymer here consisting of a poly(norbornene) backbone and poly((±)-lactide) side chains, we may assume that the plateau modulus of the poly(norbornene) backbone is lower than the plateau modulus of the poly((±)-lactide) macromonomer. This is in line with the expected decreased chain flexibility of poly(norbornene) in comparison to poly((±)-lactide). We note that Haugan et al. [22] reported a value of $G_N^0 \cong 300$ kPa for a series of poly(norbornene) homopolymers with 500–900 repeat units, in good agreement with the value for G_D found here. We also note that as seen from Table I, the plateau modulus G_N^0 of the copolymers with $N_{bb} \geq 200$ is lower than the plateau modulus of the macromonomer, which may be caused by the effect of longer poly(norbornene) backbones.

Hyperstretching for the copolymers with $N_{bb} = 320$ (Fig.9) and 420 (Fig.10) is observed at large Wi_d, while it vanishes at low Wi_d. The effect of hyperstretching is demonstrated in Fig.10 for $N_{bb} = 420$ by comparing predictions without hyperstretching ($k = 0$) to predictions with hyperstretching according to Eq.(12). At small strain rates and therefore longer time scales, hierarchical relaxation and dynamic dilution reduce the number of entanglements of the side chains along the backbone significantly, while with increasing Wi_d and on shorter time scales, more and more constraints by side chains are still active and lead to strain hardening at strain rates above the inverse of the maximal relaxation time.

Fig. 11 shows the dependence of the dilution modulus G_D as a function of the disengagement time τ_d and the number N_{bb} of repeat units of the backbone, respectively. G_D increases initially linearly with τ_d and with the 3rd power of the length of the backbone before reaching the value of the plateau modulus of the poly(norbornene) backbone, and can be described (considering the few data points tentatively) by the relations $G_D = G_N^0[1 - \exp(-(\tau_d/25s))]$ (Fig.11a) and $G_D = G_N^0[1 - \exp(-(N_{bb}/200))^3]$ (Fig.11b) with plateau modulus G_N^0 = 250 kPa.

The normalized steady-state elongational viscosity η_E/η_0 is plotted in Fig. 12a as a function of Weissenberg number $Wi_d = \dot{\varepsilon}\tau_d$ for the poly (norbornene/lactide) copolymers investigated. Lines are calculated by the HMMSF model and symbols indicate the calculated values at the experimental strain rates. Note that this is a temperature-invariant representation. While for the star-type copolymer with N_{bb}=50 the elongational viscosity decreases continously with increasing Wi_d, the bottlebrush copolymers show an opposite trend. The extensional thickening of the bottlebrush melts becomes more profound as N_{bb} increases and, therefore, the length of the backbone increases. Extensional thickening starts at $Wi_d \geq 0.2$, and up to $Wi_d \cong 0.5$, the increase is the same for all bottlebrush copolymers. The maximal value of the normalized elongational viscosities $(\eta_E/3\eta_0)_{max}$ measured increases in good approximation linearly with the number of backbone repeat units N_{bb} as shown in Fig. 12b.

5. Conclusions

Zografos et al. [7] attributed the strain hardening of the bottlebrush

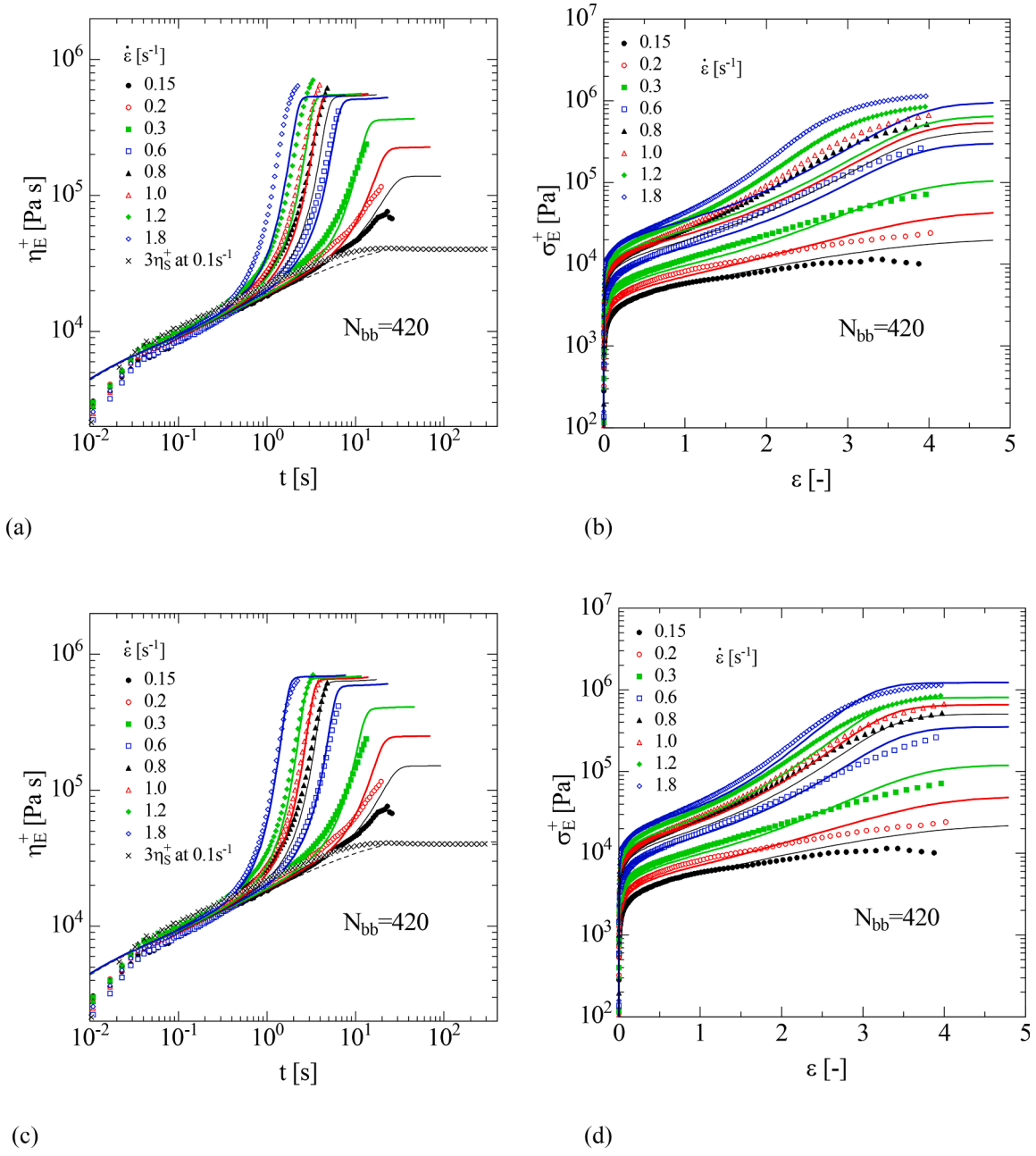

Fig. 10. Comparison of (a and c) the elongational stress growth coefficient $\eta_E^+(t)$ and (b und d) the elongational stress growth $\sigma_E^+(\varepsilon)$ data (symbols) at T_e=110 °C to calculated results of the HMMSF model (lines) with dilution modulus G_D=250 kPa, without hyperstretching (k = 0) (a and b) and with hyperstretching (c and d) acccording to Eq.(12) for copolymer with N_{bb}=420. Broken line in (a and c) is the linear-viscoelastic elongational start-up stress growth coefficient $\eta_E^0(t)$.

poly(norbornene/lactide) copolymers to an increase in side-chain interdigitation when the backbone aligns in the flow direction. They postulated an increase in intermolecular friction by side chain interaction. The concept of side-chain interdigitation was originally proposed by López-Barrón et al. [5] to give a qualitative rationalization of the elongational viscosity of poly(α-olefin) bottlebrush polymers with entangled backbone and unentangled side chains. However, Wagner and Hirschberg [8] showed that the rheology of the poly(α-olefins) can be explained by self-dilution of the backbone by the alkane side chains and that it is similar to the rheology of solutions of high molecular weight linear polymers. In contrast to the poly(α-olefin) bottlebrushes, the poly (norbornene/lactide) copolymers considered here have entangled poly ((±)-lactide) side chains and unentangled poly(norbornene) backbones. In this case, side-chain interdigitation is actually equivalent to side-chain entanglements, which are already present at equilibrium. Whereas there is no self-entanglement of the backbone, i.e. there are no direct backbone-backbone entanglements, the poly(norbornene) backbones are constrained by the entangled poly((±)-lactide) side chains. The backbone chains relax by constraint release of the side chains, and at longer times the backbone relaxes by Rouse relaxation, which occurs on the time scale of the longest relaxation time τ_{max}. It is important to note that the constraint release process is facilitated by hierarchical relaxation and dynamic dilution, i.e. the side chains already relaxed ("hierarchical relaxation") act as diluent for the chains not yet relaxed ("dynamic dilution") as, e.g., reviewed by Dealy and Larson [2]. Thus, instead of the "permanent" dilution of the backbones of the poly (α-olefin) bottlebrush polymers due to unentangled side chains [8], the backbones of the bottlebrush poly(norbornene/lactide) copolymers undergo dynamic dilution. This dynamic process takes place over a wide time range characterized by the relaxation times $\tau_i > \tau_D$ of the relaxation

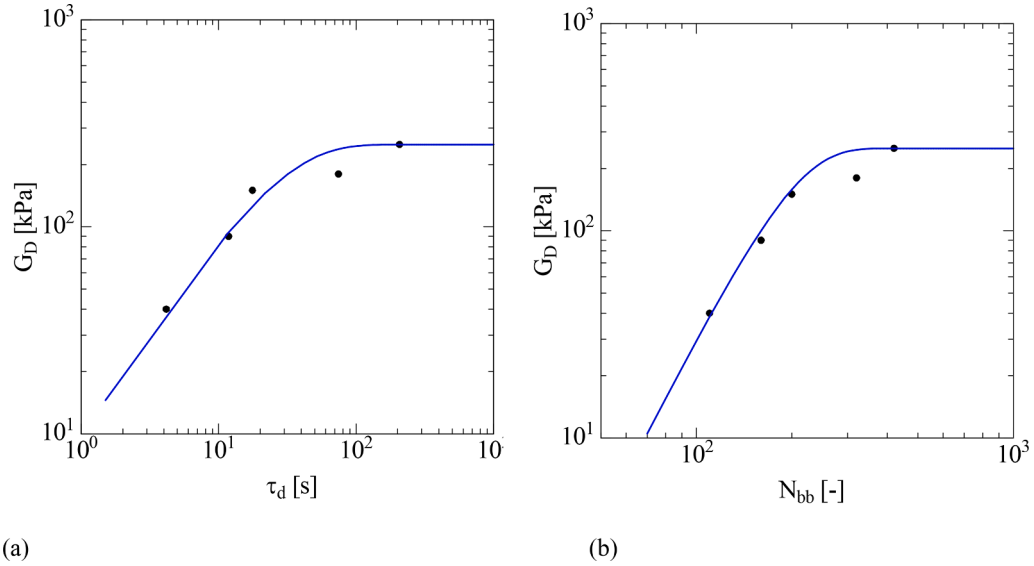

Fig. 11. Dilution modulus G_D as a function of disengagement time τ_d (a) and number N_{bb} of repeat units of the backbone (b).

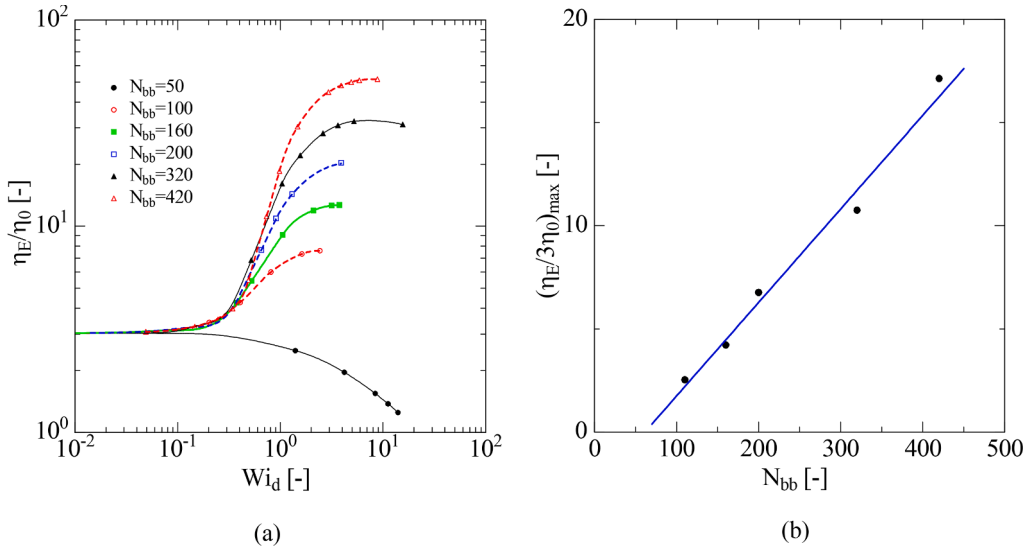

Fig. 12. (a) Normalized elongational viscosity η_E/η_0 as a function of Weissenberg number Wi_d for poly(norbornene/lactide) copolymers. (b) Maximal values of the normalized elongational viscosity $(\eta_E/3\eta_0)_{max}$ measured as a function of repeat units N_{bb} (Line with slope of 1 is a guide to the eye).

time spectrum as quantified by the HMMSF model. In nonlinear viscoelastic flows with elongation rates larger than the inverse of τ_{max}, the effect of dynamic dilution is increasingly reduced with increasing elongation rate $\dot{\varepsilon}$ due to the reduced time scale, and relaxation modes with $\tau_i > 1/\dot{\varepsilon}$ are no longer dynamically diluted. Therefore, the poly (norbornene) backbone chains are not only aligned in the flow direction but are increasingly stretched via the undiluted constraints with relaxation times $\tau_i > 1/\dot{\varepsilon}$. Thus, the postulated "increase in side-chain interdigitation" leading to strain hardening of the bottlebrush poly (norbornene/lactide) copolymers is in fact caused by a reduction of the effect of dynamic dilution with increasing deformation rate. We recall that the maximal value of the normalized elongational viscosities $(\eta_E/3\eta_0)_{max}$ increases linearly with the number of backbone repeat units N_{bb} as shown in Fig. 12b. Strain hardening is therefore resulting from orientation and stretch of the backbone chains with longer backbone chains leading to larger strain hardening.

In conclusion, the HMMSF model allows for a quantitative modeling of the elongational viscosity of the bottlebrush poly(norbornene/lactide) copolymers. The dynamically diluted weight fractions w_i of the relaxation modes are determined by considering the relaxation modulus $G(t)$ according to Eq.(11). The effect of the topology on the relaxation of side arms and backbone and their complex interactions are fully represented by the linear-viscoelastic relaxation time spectrum. We take $G(t)$ from the experimental linear-viscoelastic characterization here, but we remark that in principle, any molecular or coarse-grained model could be employed, provided it reproduces $G(t)$ quantitatively. In addition to the relaxation modulus $G(t)$, the modeling of hierarchical relaxation and dynamic dilution needs only one material parameter, the dilution modulus G_D, which increases with the disengagement time τ_d and the number N_{bb} of repeat units of the backbone before reaching the value of the plateau modulus of poly(norbornene). The effect of decreasing dynamic dilution with increasing flow rate is taken into account by implementing the weight fractions w_i in the stretch evolution Eq. (10) resulting in higher stretches for more dilute relaxation modes.

If the length of the poly(norbornene) backbone is sufficiently large, hyperstretching is observed at higher Weissenberg numbers $Wi = \dot{\varepsilon}\tau_d$, i.e., the stress growth is larger than expected for affine stretch. A similar hyperstretching behavior has been found for PS comb polymers recently,

if the number of entangled side chains per entanglement length is larger than one [15].

CRediT authorship contribution statement

Manfred H. Wagner: Writing – review & editing, Writing – original draft, Software, Investigation, Formal analysis, Conceptualization. **Aristotelis Zografos:** Writing – review & editing, Methodology, Investigation, Data curation, Conceptualization. **Valerian Hirschberg:** Writing – review & editing, Validation, Formal analysis, Conceptualization.

Declaration of competing interest

The authors declare that they have no known competing financial interests or personal relationships that could have appeared to influence the work reported in this paper.

Data availability

Data will be made available on request.

Supporting Material

This file reports the parsimonious relaxation spectra of all polymer samples investigated.

Acknowledgements

The authors would like to thank Prof. Frank S. Bates, Prof. Marc A. Hillmyer, Helena A. All, and Dr. Alice B. Chang for providing open access to the experimental data used in these analyses.

Supplementary materials

Supplementary material associated with this article can be found, in the online version, at doi:10.1016/j.jnnfm.2024.105220.

References

[1] M. Abbasi, L. Faust, M. Wilhelm, Comb and Bottlebrush Polymers with Superior Rheological and Mechanical Properties, Advanced materials (Deerfield Beach, Fla.) 31 (26) (2019) e1806484, https://doi.org/10.1002/adma.201806484. Published Online: Feb. 21, 2019.
[2] J.M. Dealy, R.G. Larson, Structure and Rheology of Molten Polymers: From structure to Flow Behavior and Back Again, Hanser Gardner Publications, Cincinnati, Ohio, USA, 2006, https://doi.org/10.3139/9783446412811.
[3] T.C.B. McLeish, R.G. Larson, Molecular constitutive equations for a class of branched polymers: the pom-pom polymer, J. Rheol. (N. Y. N. Y) 42 (1) (1998) 81–110, https://doi.org/10.1122/1.550933.
[4] M. Abbasi, L. Faust, K. Riazi, M. Wilhelm, Linear and Extensional Rheology of Model Branched Polystyrenes: from Loosely Grafted Combs to Bottlebrushes, Macromolecules. 50 (15) (2017) 5964–5977, https://doi.org/10.1021/acs.macromol.7b01034.
[5] C.R. López-Barrón, A.H. Tsou, J.R. Hagadorn, J.A. Throckmorton, Highly Entangled α-Olefin Molecular Bottlebrushes: melt Structure, Linear Rheology, and Interchain Friction Mechanism, Macromolecules. 51 (17) (2018) 6958–6966, https://doi.org/10.1021/acs.macromol.8b01431.
[6] C.R. López-Barrón, M.E. Shivokhin, J.R. Hagadorn, Extensional rheology of highly-entangled α-olefin molecular bottlebrushes, J. Rheol. (N. Y. N. Y) 63 (6) (2019) 917–926, https://doi.org/10.1122/1.5110557.
[7] A. Zografos, H.A. All, A.B. Chang, M.A. Hillmyer, F.S. Bates, Star-to-Bottlebrush Transition in Extensional and Shear Deformation of Unentangled Polymer Melts, Macromolecules. 56 (6) (2023) 2406–2417, https://doi.org/10.1021/acs.macromol.3c00015.
[8] M.H. Wagner, V. Hirschberg, Rheology of Poly(α-olefin) Bottlebrushes: effect of Self-Dilution by Alcane Side Chains, Macromolecules 57 (5) (2024) 2110–2118, https://doi.org/10.1021/acs.macromol.3c02430.
[9] M.H. Wagner, E. Narimissa, A new perspective on monomeric friction reduction in fast elongational flows of polystyrene melts and solutions, J. Rheol. (N. Y. N. Y) 65 (6) (2021) 1413–1421, https://doi.org/10.1122/8.0000345.
[10] E. Narimissa, M.H. Wagner, Review of the hierarchical multi-mode molecular stress function model for broadly distributed linear and LCB polymer melts, Polym. Eng. Sci. 59 (3) (2019) 573–583, https://doi.org/10.1002/pen.24972.
[11] E. Narimissa, M.H. Wagner, Review on tube model based constitutive equations for polydisperse linear and long-chain branched polymer melts, J. Rheol. (N. Y. N. Y) 63 (2) (2019) 361–375, https://doi.org/10.1122/1.5064642.
[12] M.H. Wagner, V. Hirschberg, Experimental validation of the hierarchical multi-mode molecular stress function model in elongational flow of long-chain branched polymer melts, J. Nonnewton. Fluid. Mech. 321 (2023) 105130, https://doi.org/10.1016/j.jnnfm.2023.105130.
[13] V. Hirschberg, M.G. Schusmann, M.C. Ropert, M. Wilhelm, M.H. Wagner, Modeling elongational viscosity and brittle fracture of 10 polystyrene Pom-Poms by the hierarchical molecular stress function model, Rheol. Acta 62 (2023) 269–283, https://doi.org/10.1007/s00397-023-01393-0.
[14] V. Hirschberg, S. Lyu, M.G. Schußmann, M. Wilhelm, M.H. Wagner, Modeling elongational viscosity of polystyrene Pom-Pom/linear and Pom-Pom/star blends, Rheol. Acta 62 (2023) 433–445.
[15] V. Hirschberg, L. Faust, M. Abbasi, Q. Huang, M. Wilhelm, M.H. Wagner, Hyperstretching in Elongational Flow of Densely Grafted Comb and Branch-on-Branch Model Polystyrenes, J. Rheol. 68 (2024) 229–246.
[16] L. Poh, E. Narimissa, M.H. Wagner, H.H. Winter, Interactive Shear and Extensional Rheology—25 years of IRIS Software, Rheol. Acta 61 (4–5) (2022) 259–269, https://doi.org/10.1007/s00397-022-01331-6.
[17] H.H. Winter, M. Mours, The cyber infrastructure initiative for rheology, Rheol. Acta 45 (4) (2006) 331–338, https://doi.org/10.1007/s00397-005-0041-7.
[18] D.R. Witzke, Introduction to properties, Engineering and Prospects of Polylactide Polymers, PhDChemical Engineering, Michigan State University, 1997.
[19] M. Doi, S.F. Edwards, Dynamics of concentrated polymer systems. Part 4.—Rheological properties, J. Chem. Soc., Faraday Trans. 75 (0) (1979) 38–54, https://doi.org/10.1039/F29797500038. *2*.
[20] M. Doi, S.F. Edwards, Dynamics of concentrated polymer systems. Part 3.—The constitutive equation, J. Chem. Soc., Faraday Tras. 74 (0) (1978) 1818–1832, https://doi.org/10.1039/F29787401818. *2*.
[21] E. Narimissa, V.H. Rolón-Garrido, M.H. Wagner, A hierarchical multi-mode MSF model for long-chain branched polymer melts part I: elongational flow, Rheol. Acta 54 (9–10) (2015) 779–791, https://doi.org/10.1007/s00397-015-0879-2.
[22] I.N. Haugan, M.J. Maher, A.B. Chang, T.P. Lin, R.H. Grubbs, M.H. Hillmyer, F. S. Bates, Consequences of Grafting Density on the Linear Viscoelastic Behavior of Graft Polymers, ACS. Macro Lett. 7 (2018) 525–530.